ELSEVIER

Journal of Photochemistry and Photobiology A: Chemistry 133 (2000) 159–167

Journal of Photochemistry and Photobiology A:Chemistry

www.elsevier.nl/locate/jphotochem

Nanosecond UV laser photoionization of aqueous tryptophan: temperature dependence of quantum yield, mechanism, and kinetics of hydrated electron decay

Kenneth L. Stevenson [a,*], George A. Papadantonakis [b], Pierre R. LeBreton [b]

[a] *Department of Chemistry, Indiana University-Purdue University Fort Wayne, Fort Wayne, IN 46805, USA*

[b] *Department of Chemistry, University of Illinois at Chicago, 845 W. Taylor Street, Chicago, IL 60607, USA*

Received 30 July 1999; received in revised form 3 February 2000; accepted 7 February 2000

Abstract

The 266 nm photoionization of aqueous tryptophan (Trp) solution at natural pH has been studied by laser flash photolysis using 3–18 mJ, 7 ns, 266 nm pulses. The transient absorption method was employed to detect hydrated electrons. The photoionization mechanism is a combination of mono and biphotonic processes. Results from measurements of the power dependence of photoionization and of triplet (T_1) state production suggest that both processes involve the same one-photon and two-photon singlet intermediate state. The hydrated electron yield increases with temperature, and this can be attributed primarily to the monophotonic photoionization component. Hydrated electrons decay by a non-exponential rate law that is consistent with a decay mechanism involving their bimolecular scavenging by tryptophan radical cations with a rate constant of $(7.2\pm0.6)\times10^{10}\ M^{-1}\ s^{-1}$.

Keywords: Photodegradation; Tryptophan; Triplet

1. Introduction

The photodegradation of tryptophan plays an important role in the UV induced inactivation of proteins, and a major tryptophan photodegradation pathway involves photoionization [1–5]. For this reason the photoionization of aqueous tryptophan [6–10] and of its chromophore (indole) [11–18] has been widely investigated. In early electron scavenging experiments employing conventional continuous wave (CW) mercury and xenon lamps the single-photon ionization of indole and tryptophan was reported for wavelengths shorter than 275 nm [6,11,12]. Several, more recent experiments employed 266 nm excitation together with transient absorption detection of the hydrated electrons. Bent and Hayon, in an early 266 nm laser photolysis experiment [7], using 20–25 mJ, 15 ns pulses reported that tryptophan undergoes primarily one-photon photoionization with a small biphotonic contribution. In these experiments, the laser beam and the analyzing beam were perpendicular. Later, Lachish et al. [9] reported that with low intensity, 266 nm, 20 ns, 2 mJ laser pulses tryptophan photoionization occurs primarily via a two-photon process. In these experiments, the laser beam and the analyzing beam were collinear. Grossweiner et al. [17] employing a perpendicular configuration, and a combination of 265 nm, 17 ns, 20 mJ with 530 nm, 17 ns, 60 mJ laser pulses found that the 266 nm photoionization is enhanced by excited state absorption of 530 nm photons. Other two-pulse experiments, using the perpendicular configuration and combinations of 266 with 353 or 530 nm photons at low energies (1.2 to 1.7 mJ pulses of 1 to 20 ns duration), support the conclusion that at low laser power both monophotonic and biphotonic tryptophan photoionization occurs [10].

An interesting and controversial feature of tryptophan and indole photoionization is the reported increase of the photoionization quantum yield (ϕ_{e^-}) with temperature in the range 10 to 80°C. As first reported by Feitelson [11], in a CW electron-scavenging experiment using 254 nm excitation, a 3-fold increase of ϕ_{e^-} for indole occurs as the temperature increases from 10 to 45°C. Similar results for indole and tryptophan were obtained by Bent and Hayon in subsequent 266 nm laser experiments [7] in which photoionization was monitored by measuring the transient absorbance of hydrated electrons at 720 nm. For tryptophan, the increase of ϕ_{e^-} with temperature was confirmed by Robbins et al. [8], in an investigation of the temperature dependence of

* Corresponding author.

1010-6030/00/$ – see front matter
PII: S1010-6030(00)00235-5

the fluorescence decay kinetics of aqueous tryptophan as a function of temperature. In the combination of one- and two-photon photoionization mechanisms reported by Grossweiner et al. [17] the quantum yield for one-photon photoionization was found to increase with temperature. More recent results [19,20] from 240–320 nm picosecond laser measurements of the temperature dependence of the fluorescence quantum yield of indole have cast doubt on the earlier observations of the temperature dependence of ϕ_{e-} [7], using the argument that the temperature increase of the indole photoionization quantum yield may be due to an increase in the ground-state absorbance with temperature.

In addition to questions concerning whether 266 nm laser photoionization of tryptophan is a one- or two-photon process, and whether the photoionization quantum yield increases with temperature, a third area of interest involves the kinetics for decay of the solvated electrons produced by photoionization. Femtosecond laser kinetic investigations [16] of indole at 260 nm demonstrated that over time ranges as large as 100 ps there was no observable decay of solvated electrons formed in the photoionization process, indicating that geminate recombination is insignificant on this time scale.

The goals of the present investigation are: (a) to further compare and quantify the one-versus two-photon ionization of tryptophan by nanosecond pulsed laser experiments at 266 nm, (b) to review the temperature dependence of the photoionization quantum yield and (c) to examine the decay kinetics of the hydrated electrons formed via photoionization.

2. Materials and methods

L-Tryptophan MicroSelect grade was obtained from Fluka and used as received. Corning mega pure system MP-1 provided doubly distilled water for all solutions. Absorption spectra were measured on a Perkin Elmer Lambda 6 spectrophotometer and on a Hewlett Packard 8452A diode array spectrophotometer equipped with a Hewlett Packard 89090A thermostat. The tryptophan solutions were unbuffered and had a natural pH 5.9.

Flash photolysis of aqueous solutions was carried out at room temperature in a 1 cm cuvette, which in most cases was a flow-through type. Before photolysis, 100 ml of each solution was bubbled with Ar gas (itself purged of oxygen by bubbling through chromous chloride and potassium hydroxide solutions) for at least 30 min to remove oxygen. The irradiating source was the unfocused 266 nm beam of a Surelite Nd-YAG laser of 7 ns nominal pulse width. For determining time-resolved absorption spectra, the light monitoring system consisted of a 75 W Xe arc lamp (Photon Technology International), pulsed by a laser diode driver (Analog Modules). The 266 nm laser pulse was reflected into the sample cuvette using a dichroic mirror transparent to the analyzing beam so that both beams were as nearly collinear as possible. After leaving the sample, the analyzing light beam was admitted to the entrance slit of a monochromator (Photon Technology International), equipped at the exit slit with a Hammamatsu R936 photomultiplier, which has extended red sensitivity. The photomultiplier signal was captured and processed by a Hewlett Packard 54510 oscilloscope, and stored on computer disk, via National Instruments' LabWindows software, for later processing. Time-resolved spectra were obtained by capturing single-shot signals at a series of wavelengths and storing and processing the absorbances at predetermined delay times after the flash. For sensitive monitoring of the electron decays, a 5 mW, 670 nm diode laser (Thorlabs) was substituted for the arc lamp in order to obtain signals with high *S*/*N* ratio. Power studies of various transients were accomplished by capturing sample transient signals at varying laser power supply voltages and comparing their amplitudes to the maximum 670 nm absorbance in 0.001 M sodium ferrocyanide, ($Na_4Fe(CN)_6$), which photoejects hydrated electrons monophotonically at 266 nm with a known quantum yield of 0.52 [21]. Shot-to-shot intensity stability was maintained by simmering the laser flashtube at 1 Hz. No correction for the partial absorption of laser pulses was necessary for either tryptophan or ferrocyanide solutions. In both cases, the absorbance at 266 nm was 2.0, ensuring that more than 99% of all photons were absorbed. Transient signals for kinetic analysis were in most cases obtained by taking the average of three shots.

3. Results and discussion

3.1. One- and two-photon ionization

Fig. 1 shows absorbances (A_{Trp}) measured at 670 nm and 23.6°C, for hydrated electrons formed in the 266 nm laser photoionization of 5×10^{-4} M tryptophan. The laser energies are represented by the absorbances ($A_{Na_4Fe(CN)_6}$) at 670 nm of electrons produced in the monophotonic photoionization of a 0.001 M sodium ferrocyanide solution [21]. Values of both A_{Trp} and $A_{Na_4Fe(CN)_6}$ were obtained from transient absorption signals extrapolated to zero delay time. The nonlinearity of the curve in Fig. 1 provides evidence that the electron is produced at least partially by a biphotonic process. If both one- and two-photon ionization occurs then the electron absorbance should have two components: one proportional to $A_{Na_4Fe(CN)_6}$ and another proportional to $A^2_{Na_4Fe(CN)_6}$ such that,

$$A_{Trp} = \alpha A_{Na_4Fe(CN)_6} + \beta A^2_{Na_4Fe(CN)_6} \quad (1)$$

A least squares fit of Eq. (1) to the data in Fig. 1 results in values of 0.072 and 0.374 for α and β, respectively. Since the net photoionization quantum yield (ϕ_{net}) is given by

$$\phi_{net} = \phi_1 + \phi_2 \quad (2)$$

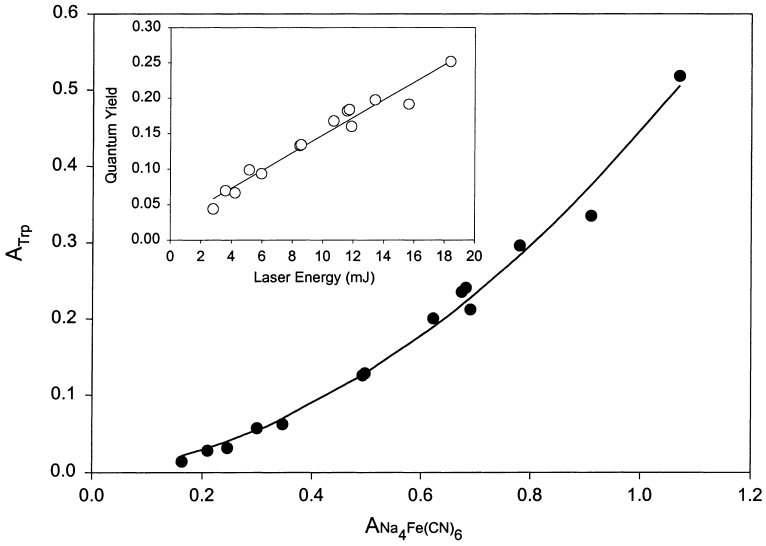

Fig. 1. Plot of the absorbance of hydrated electrons produced from 266 nm laser photoionization of 5×10^{-4} M tryptophan vs. the laser pulse energy measured as the 670 nm absorbance of electrons produced from monophotonic ionization of 0.001 M sodium ferrocyanide. The solid line is a least-squares fit to Eq. (1). Inset: plot of the quantum yield for hydrated electron production vs. the energy of the laser pulse, with linear regression line.

where ϕ_1 and ϕ_2 are the quantum yields for mono- and biphotonic photoionization, respectively, and since the quantum yield for photoionization of ferrocyanide is 0.52 [21], the value of α can be used to calculate the monophotonic yield, ϕ_1=0.52α. This results in a monophotonic quantum yield at 23.6°C of 0.037±0.009, which compares favorably to 0.04 obtained by Finnström et al. [10] for tryptophan at approximately the same temperature. The inset to Fig. 1 shows the linear dependence of ϕ_{net} on the laser energy

By employing the relationship

$$\phi_{net} = 0.52\frac{A_{Trp}}{A_{Na_4Fe(CN)_6}} \quad (3)$$

together with a ϕ_1 value of 0.037, and Eq. (2), the percentage of electrons observed from one-photon ionization can be estimated as a function of laser power. These values are given in Table 1. The results indicate that, as the power increases from 2.8 to 18.4 mJ, the percentage of electrons produced via one-photon photoionization decreases from 85 to 15%.

Table 1
Percentage of electrons formed via one-photon 266 nm tryptophan photo-ionization[a]

Laser energy (mJ)	Percent
2.8	85
3.6	54
5.9	40
8.4	29
8.5	28
10.6	22
13.4	19
18.4	15

[a] Measured with collinear excitation and absorption optics at 25°C, See text.

The relative contribution of one- versus two-photon photoionization depends heavily on the experimental configuration. If the analyzing beam is at right angles to the laser beam, a double logarithmic plot of electron absorbance versus laser intensity has a smaller slope than if the analyzing and laser beams are collinear. This can be explained in terms of differences in the photoionization sampling regions associated with the two configurations. As the laser beam is attenuated when it passes through the solution, biphotonic photoionization decreases nonlinearly along the path. In the perpendicular configuration, the analyzing beam samples photoionization at some distance from the irradiated face of the cell, whereas in the collinear experiment, the analyzing path is essentially the same as that of the laser beam such that more biphotonic events are sampled than in the perpendicular configuration.

3.2. Temperature dependence

Fig. 2 contains a plot of 670 nm absorbance versus temperature (closed squares) for hydrated electrons formed via photoionization of 5×10^{-4} M tryptophan with 2.4 mJ, 266 nm pulses. The figure also shows the temperature dependence of the 266 nm absorbances of 5×10^{-4} M tryptophan (closed circles) and 3.2×10^{-4} M indole (open squares). Finally, Fig. 2 contains data (closed triangles) showing that the extinction coefficient of the hydrated electron at 670 nm decreases with temperature [22]. For tryptophan, the results indicate a substantial increase of hydrated electrons occurs in the temperature range, 11 to 82°C, while the 266 nm absorbance remains essentially constant. For indole, the 266 nm absorbance decreases slightly with increasing temperature. These results demonstrate that the increase in the 266 nm photoioniza-

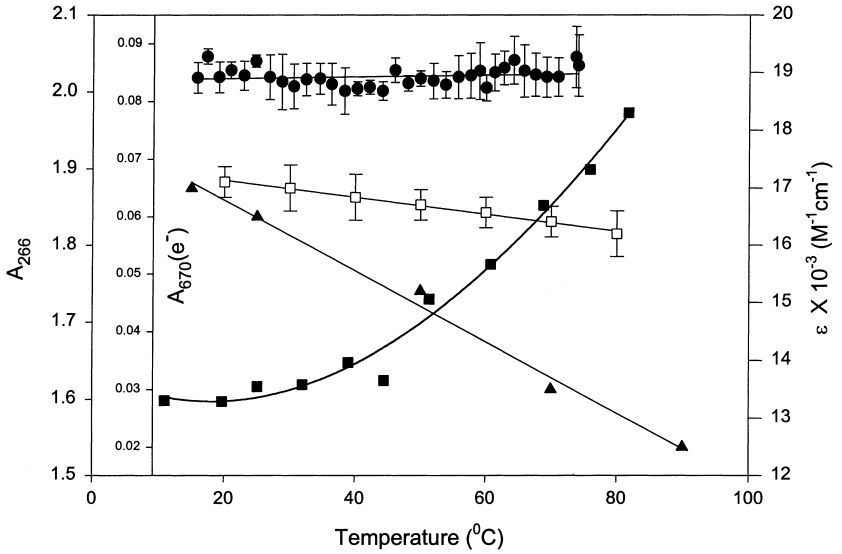

Fig. 2. Plot of 670 nm absorbance (■) of electrons formed via photoionization of 5×10^{-4} M tryptophan with 266 nm, 2.4 mJ pulses vs. temperature. Absorbance measurements correspond to the initial intensity obtained by extrapolation of the transient absorbance signal to a delay time of 0. Absorbance of $5\times x10^{-4}$ M tryptophan (●) and 3.5×10^{-4} M indole (□) at 266 nm vs. temperature. The figure also shows a plot of the extinction coefficient (▲) of the hydrated electron at 670 nm vs. temperature. The scale for the 670 nm absorbance of solvated electrons formed from tryptophan photoionization is given inside the border on the left. The scale for the 266 nm absorbances of tryptophan and indole is given outside the border on the left. The scale for the 670 nm extinction coefficients of solvated electrons is given on the right. The solid lines are guides for the eye.

tion quantum yield of tryptophan, and that reported earlier for indole [7], are not due to increases in absorbance with temperature.

A series of power studies was carried out at different temperatures from 13.6 to 75.5°C so that the parameter α, could be determined as a function of temperature from fits to Eq. (1). The results in Fig. 3, corrected for the change in the electron extinction coefficient with temperature, indicate that the monophotonic quantum yield increases about fivefold in this temperature range, essentially accounting for the temperature effect observed in Fig. 2. These results are consistent with the earlier report [17] that, while tryptophan photoionization has both mono- and biphotonic components, it is the monophotonic step that is temperature dependent. Furthermore, the observation that tryptophan and indole fluorescence decrease in the same temperature range [8,11] is consistent with the conclusion that the excited singlet state S_1, produced by one-photon absorption is the precursor of the hydrated electron. It has been suggested [10] that S_1 is also the primary source of the biphotonic electron

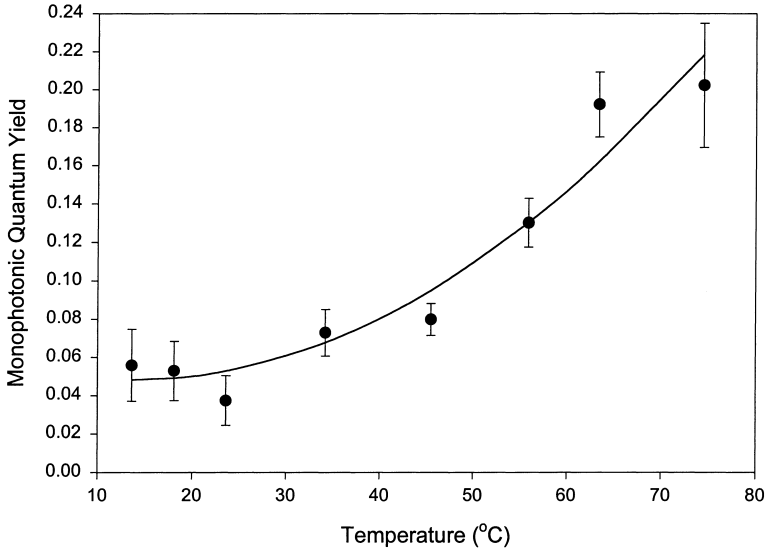

Fig. 3. Quantum yield of monophotonic, 266 nm photoionization of 5×10^{-4} M tryptophan as a function of temperature. The solid line is a guide for the eye.

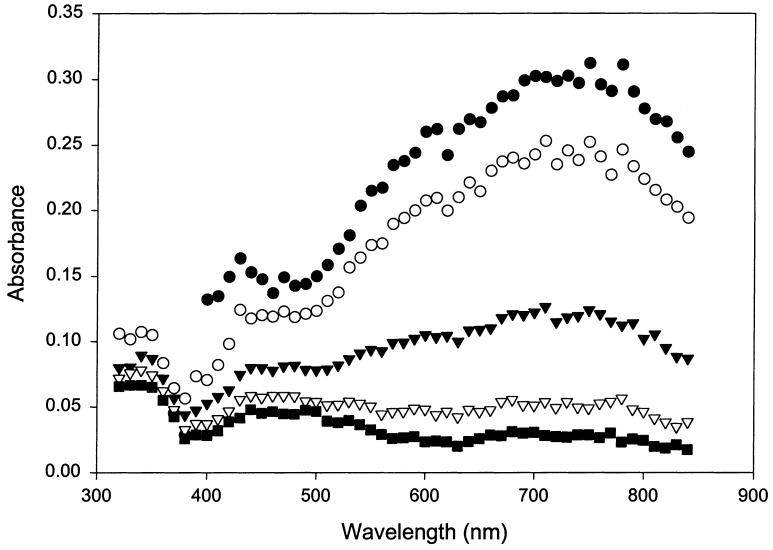

Fig. 4. Transient absorption spectra of 5×10^{-4} M tryptophan measured after irradiation with 266 nm, 18 mJ pulses. Spectra measured at delay times of 40 ns (●), 100 ns (○), 400 ns (▼), 1000 ns (▽), and 1700 ns (■) are shown. The 40 ns spectrum has been truncated due to noise in the 300–400 nm region generated by ringing from fluorescence.

ejection, based on studies in which excitation pulse widths were varied [7,10]. This mechanism is consistent with the results described below.

3.3. Transient species

Fig. 4 shows transient absorption spectra obtained from 5×10^{-4} M tryptophan at natural pH 5.9. Most of the features of these spectra have been characterized previously by other groups, including: (1) the hydrated electron which has a maximum absorption in the 700–720 nm region [23], (2) a 420 nm absorbing species identified as a triplet state, T_1 [7], (3) a 460 nm absorbing species, particularly visible at the longest delay time, assigned as another triplet, T_2 [7], and (4) a small shoulder or peak at 580 nm associated with the tryptophan cation radical, $Trp^{\bullet+}$, [24–27] formed with the electron via photoionization. The results indicate that the $Trp^{\bullet+}$ absorption is most prominent in the 40 ns spectrum, which also has the highest electron absorbance, but disappears when the electron has completely decayed. This suggests that a major decay pathway for the two species is recombination,

$$Trp^{\bullet+} + e^-_{aq} \rightarrow Trp \quad (4)$$

The importance of recombination is confirmed by the results in Fig. 5, which shows transient spectra taken in 5×10^{-4} M

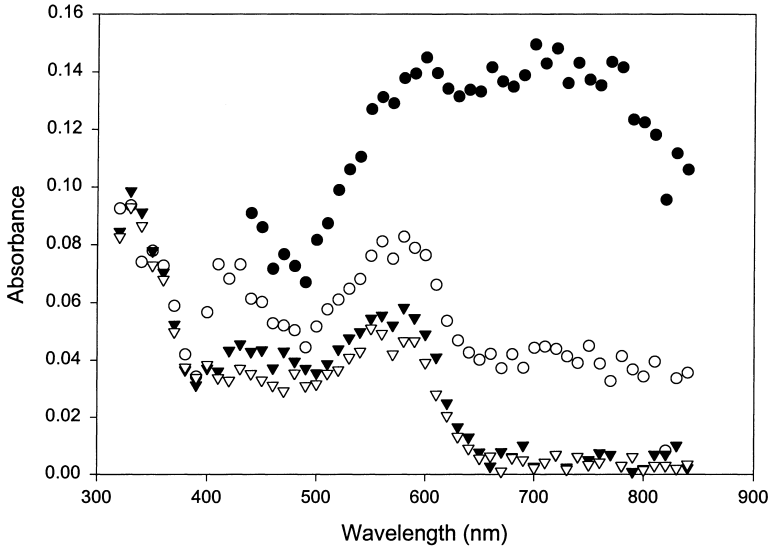

Fig. 5. Transient absorption spectra of 5×10^{-4} M tryptophan containing 1×10^{-3} M HCl, measured after irradiation with 266 nm, 18 mJ pulses. Spectra were obtained at delay times of 40 ns (●), 100 ns (○), 400 ns (▼), and 1700 ns (▽) are shown. Truncation of the 40 ns spectrum is the same as that in Fig. 4.

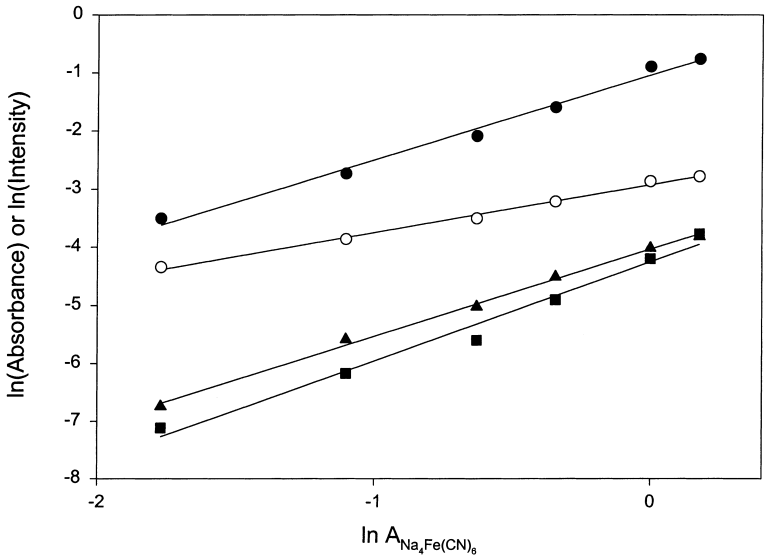

Fig. 6. Double logarithmic plots of tryptophan fluorescence intensity and initial absorbance of transient species formed via excitation of tryptophan vs. absorbance of hydrated electrons formed in 10^{-3} M $Na_4Fe(CN)_6$. Tryptophan excitation measurements were carried out at 5×10^{-4} M tryptophan in 10^{-3} M HCl with 266 nm laser pulses of varying energy. The absorbance of hydrated electrons from $Na_4Fe(CN)_6$ was measured at 670 nm. For transient species formed via tryptophan excitation the plots show (●) absorbance at 670 nm, slope=1.46 (hydrated electron); (○) fluorescence at 420 nm, slope=0.824 (S_1); (▲) absorbance at 420 nm, slope=1.50 (T_1); and (■) absorbance at 580 nm, slope=1.70 (Trp^+).

tryptophan at pH=3, where 82% of the tryptophan, with a pK_1 of 2.28 [28], exists as the zwitterion. Under such acidic conditions electron decay occurs primarily through proton scavenging,

$$H^+ + e^-_{aq} \rightarrow H^\bullet \quad (5)$$

This occurs much faster than recombination so that decay of $Trp^{\bullet+}$ is slowed and its absorption at 580 nm persists after electron decay is complete.

To determine which species are involved in two-photon ionization, a power study was made on 5×10^{-4} M tryptophan at 25°C and pH 3 and at several wavelengths. In these experiments, the initial absorbances (0-time) at 670, 580, and 420 nm, and the maximum fluorescence emission intensity at 420 nm, were measured at varying 266 nm pulse energy. Fig. 6 shows double logarithmic plots of the resulting absorbances or fluorescence intensities. A consideration of the slopes of the plots in Fig. 6 leads to several conclusions: (1) The electron (slope, 1.46) and the radical cation (slope, 1.70) are both formed via mechanisms with a two-photon component, and $Trp^{\bullet+}$ formation has a greater biphotonic cross section than electron formation. The greater two-photon character associated with $Trp^{\bullet+}$ formation is possibly due to another reaction besides electron ejection from the zwitterion, such as hydrogen atom ejection from the cationic form of tryptophan. (2) The T_1 species (slope, 1.50) is formed biphotonically to the same extent as the electron, suggesting a common precursor. (3) The fluorescence (slope, 0.82) is less than monophotonic providing evidence that the excited singlet S_1 is deactivated at higher light intensities and is the species absorbing the photon resulting in two-photon photoionization and T_1 formation.

The following mechanism is consistent with these observations:

$$S_0 + h\nu \rightarrow S_1 \quad (6)$$

$$S_1 \rightarrow Trp^{\bullet+} + e^-_{aq} \quad (7)$$

$$S_1 \rightarrow S_0 + h\nu \quad (8)$$

$$S_1 \rightarrow T_1 \quad (9)$$

$$S_1 + h\nu \rightarrow S_2 \quad (10)$$

$$S_2 \rightarrow Trp^{\bullet+} + e^-_{aq} \quad (11)$$

$$S_2 \rightarrow T_1 \quad (12)$$

Reaction 10 is the biphotonic step, for which the results in Fig. 6 indicate a common intermediate, designated S_2. This mechanism is different from one proposed earlier [17] in which two-photon ionization occurs at 265 nm via an intermediate state that is not S_1. Earlier investigations of indole and tryptophan monophotonic photoionization provide conflicting evidence [25] concerning vibrational excitation in the intermediate S_1 state. It is uncertain whether ionization to the water conduction band occurs from the ground vibrational level of S_1 [29,30] or from vibrationally excited states within the S_1 manifold [6,12,17]. The present results do not discriminate between these possibilities

3.4. Electron decay

Fig. 7 contains logarithmic plots of absorbance versus time. The figure compares the decay of the hydrated electron formed via photoionization of 5×10^{-4} M tryptophan in solution without acid (pH=5.9) to that in solution with 0.001 M

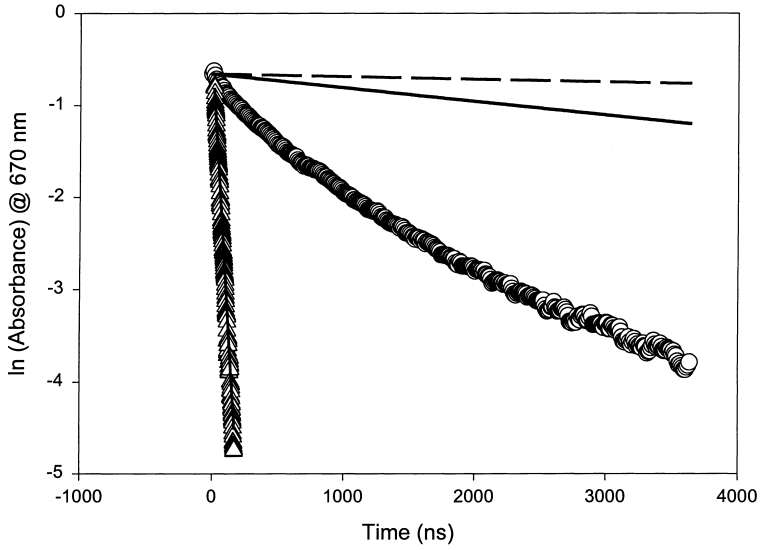

Fig. 7. Plot of the logarithm of 670 nm absorbance of hydrated electrons vs. time for photoionization of 5×10^{-4} M tryptophan (△) at a pH of 3, and (○) at a natural pH of 5.9. Calculated plots for electron decay are shown for comparison for the hypothetical situations (---) if the only electron scavenger were proton at pH 5.9 (k=2.3×10^{10} M^{-1} s^{-1}), and (—) if the only electron scavenger were neutral tryptophan (k=3×10^{8} M^{-1} s^{-1}).

HCl (pH=3). At pH 3, where the primary electron scavenger is H^+, the plot is linear and the decay is pseudo first-order. The slope of this plot (2.5×10^{7} s^{-1}) should be equal to k [H^+], yielding a value for the second-order H^+- electron scavenging constant k of 2.5×10^{10} M^{-1} s^{-1} which is in agreement with the accepted value of 2.3×10^{10} M^{-1} s^{-1} at 25°C [31].

At natural pH, the results in Fig. 7 are nonlinear suggesting that the electron decay may be described by a second-order rate law, consistent with the bimolecular recombination of Eq. (4). We have added simulated decay curves of the electron in this solution for the two hypothetical situations where proton at pH=5.9 is the only scavenger (k=2.3×10^{10} M^{-1} s^{-1}), and where neutral Trp is the only scavenger (k=3×10^{8} M^{-1} s^{-1} [27,32–34]), indicating that neither of these could account for the rapid electron decay observed. Since $Trp^{\bullet+}$ and e^-_{aq} must be formed in equal amounts by the laser pulse according to Eqs. (7) and (11), if the only electron-scavenging reaction were recombination then the decay should follow the simple second-order integrated expression,

$$\frac{1}{[e^-_{aq}]} - \frac{1}{[e^-_{aq}]_0} = kt \tag{13}$$

where $[e^-_{aq}]_0$ is the concentration of hydrated electron immediately after the excitation pulse. However, because the Trp solution at 5×10^{-4} M has such a high absorbance at the laser pulse wavelength (see Fig. 2) there is a very sharp gradient in the value of $[e^-_{aq}]$ from the front to the back of the cell, but the net absorbance of the solution at 670 nm is only an average of $[e^-_{aq}]$ times the molar extinction coefficient and cell pathlength, and thus Eq. (13) cannot accurately describe the decay of absorbance with time. This problem can be partially overcome by using Trp solutions with a much lower absorbance such that there is a small gradient in $[e^-_{aq}]$; for example at [Trp]=1×10^{-5} M the percent of incident photons absorbed in the first 1 mm of the cuvette is 0.9% compared to 0.8% in the last 1 mm, whereas in a 5×10^{-4} M solution the values are 36.9% versus 0.6%.

A series of transient absorbance decays at 670 nm were therefore taken on samples in which the tryptophan concentration was varied from 1×10^{-5} M to 9×10^{-5} M in order to optimize the conditions for second-order decay measurements. Nevertheless, it was observed that a plot of reciprocal of absorbance versus time still did not yield a straight line, as suggested by Eq. (13); rather, the plots deviated positively with time from the initial slopes. This indicated that the electron concentrations are decreased from the values they ought to have if the only scavenger is Trp^+ (Eq. (4)) and thus there must be other electron scavengers in the system, such as Trp, trace O_2 (k=1.9×10^{10} M^{-1} s^{-1} [35]), trace impurities in the tryptophan, or the electron itself ($2k$=1×10^{10} M^{-1} s^{-1} [35]).

To a first approximation, the system can be treated as though it consists of two parallel reactions, the first of which is the recombination reaction of Eq. (4) with rate constant k_2, and the second of which is a pseudo first-order decay of the electron with net rate constant k_1 which incorporates all of the other scavenging processes, assumed to be slower than the recombination. The differential rate equations for such a system of parallel reactions can be integrated [36], and assuming that the initial concentrations of Trp^+ and e^-_{aq} are equal as a result of the photoionization, the following expression results for a 1 cm pathlength:

$$\ln\left\{\frac{(k_1/k_2 + A/\varepsilon)A_0}{(k_1/k_2 + A_0/\varepsilon)A}\right\} = k_1 t \tag{14}$$

where A is the absorbance, A_0 the initial absorbance, and ε

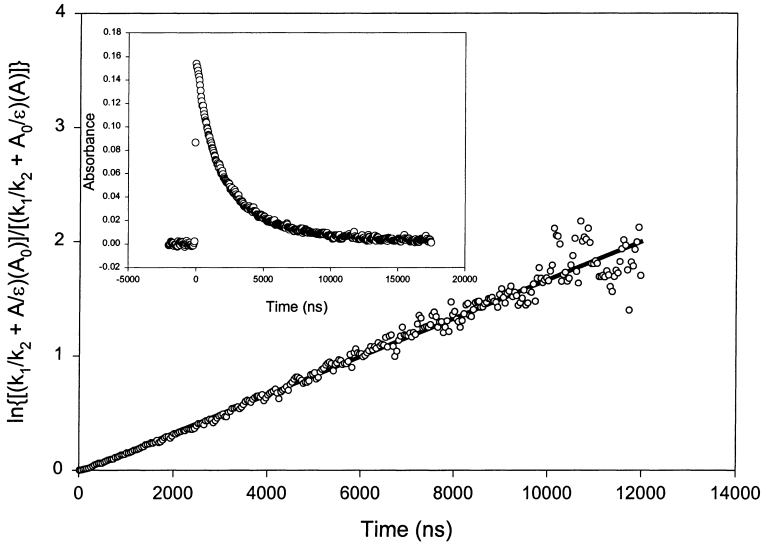

Fig. 8. Plot of the left side of Eq. (14) vs. time, with linear regression line, for a solution of 1.96×10^{-5} M tryptophan, exposed to a 266 nm laser flash, using the value of ε=18100 M^{-1} cm^{-1}, the optimum value of $k_1/k_2=2.4\times10^{-6}$ M, resulting in a slope of 1.67×10^{5} s^{-1} and a value of $k_2=7.0\times10^{10}$ M^{-1} s^{-1}. Inset: the raw absorbance vs. time data.

the molar extinction coefficient of the electron at the monitoring wavelength. A value of k_1/k_2 can be found that gives the best linear fit (as indicated by the closest value of the correlation coefficient to 1) of the plot of the left side of Eq. (14) versus t, with the slope yielding k_1 and hence k_2. Fig. 8 shows such a linear plot using the absorbance-versus-time values shown in the inset. The measurement of 11 values of k_2 in this fashion resulted in an average value of $k_2=(7.2\pm0.6)\times10^{10}$ M^{-1} s^{-1} for the recombination reaction, Eq. (4), which is close to the diffusion-controlled limit. This result may be compared to the those of Lee et al [37] who estimate a recombination rate constant between 3.1×10^{10} and 9×10^{10} M^{-1} s^{-1}. The pseudo first-order rate constants varied from 1×10^{5} to 3×10^{5} s^{-1} in the concentration range of 0 to 8×10^{-5} M tryptophan. This would result in a second-order rate constant for scavenging of electron by tryptophan of about 2.5×10^{9} M^{-1} s^{-1} which is about 10 times the value reported earlier [27,32–34]. Thus, our results indicate that in the present experiments, neutral Trp is not the principal contributor to the second pseudo first-order decay pathway.

A recent investigation [18] of the time dependence of conductivity following 193 nm photoionization of tryptophan solutions at a pH of 8.3 provided evidence that significant deprotonation of the tryptophan radical cation occurs at times less than 1000 ns. The observation that the addition of the electron scavenger, N_2O had little influence on the conductivity time dependence, led to the speculation that $Trp^{\bullet+}$ recombination with e^-_{aq} occurs on a time scale greater than 1000 ns. A consideration of the 266 nm results obtained at a pH of 5.9 which are shown in Fig. 7 indicates that neither H^+ scavenging nor scavenging by neutral tryptophan can account for the significant decay of the e^-_{aq} concentration at times less than 1000 ns. This observation is consistent with the conclusion that, in the present experiments, the recombination reaction occurs rapidly on a time scale less than 1000 ns.

4. Conclusions

1. The photoionization of aqueous tryptophan occurs by a combination of monophotonic and biphotonic absorption. With 2.8 mJ, 266 nm pulses, 85% of the electrons detected at 25°C in a collinear configuration are formed via a one-photon mechanism. With 18.4 mJ pulses, 85% of the electrons are formed via a two-photon mechanism.
2. The monophotonic photoionization quantum yield increases more than fourfold as the temperature increases from 11 to 82°C.
3. In addition to photoionization, the population of the first excited triplet state of tryptophan occurs via a mixture of one- and two-photon mechanisms. The finding that photoionization and T_1 population exhibit similar laser power dependence suggests that the mechanisms employ the same intermediate singlet state.
4. At natural pH (5.9), tryptophan photoelectrons are primarily scavenged by tryptophan radical cations at or near the diffusion limit.

Acknowledgements

Support of this work by the Petroleum Research Fund of the American Chemical Society, and by the American Cancer Society (RPG-91-024-09-CNE) is gratefully acknowledged. The authors thank Dr. Qiqing Zhu for help

in preparation of the manuscript. They also thank Kaushalya Ekanakye for measuring the temperature dependence of the absorption spectrum of tryptophan.

References

[1] A.D. McLaren, D. Shugar Photochemistry of Proteins and Nucleic Acids. MacMillan, New York, 1964.
[2] M. Bazin, J. Pierre, P. Debey, R. Santus, Eur. J. Biochem. 124 (1982) 539–544.
[3] J. Dillon, D. Roy, A. Spector, Exp. Eye Res. 41 (1985) 53–60.
[4] J.A. Shauerte, A. Gafni, Biochem. Biophys. Res. Commun. 212 (1995) 900–905.
[5] L.I. Grossweiner, Curr. Eye Res. 3 (1984) 137–144.
[6] E. Amouyal, A. Bernas, D. Grand, Photochem. Photobiol. 29 (1979) 147–155.
[7] D.V. Bent, E. Hayon, J. Am. Chem. Soc. 97 (1975) 2612–2619.
[8] R.J. Robbins, G.R. Fleming, G.S. Beddard, G.W. Robinson, P.J. Thistlethwaite, G.J. Woolfe, J. Am. Chem. Soc. 102 (1980) 6271–6279.
[9] U. Lachish, A. Shafferman, G. Stein, J. Chem. Phys. 64 (1976) 4205–4211.
[10] B. Finnström, F. Tfibel, L. Lindqvist, Chem. Phys. Lett. 71 (1980) 312–315.
[11] J. Feitelson, Photochem. Photobiol. 13 (1971) 87–96.
[12] A. Bernas, D. Grand, E. Amouyal, J. Phys. Chem. 84 (1980) 1259–1262.
[13] F. Saito, S. Tobita, H. Shizuka, J. Photochem. Photobiol A: Chem. 106 (1997) 119–126.
[14] C. Pigault, D. Gérard, G. Laustriat, in: Proceedings of 10th International Conference on Photochemistry, Iraklion, Greece, 6–12 September 1981.
[15] J.C. Mialocq, E. Amouyal, A. Bernas, D. Grand, J. Phys. Chem. 86 (1982) 3173–3177.
[16] J. Peon, G.C. Hess, J.-M.L. Pecourt, T. Yuzawa, B. Kohler, J. Phys. Chem. A 103 (1999) 2460–2466.
[17] L.I. Grossweiner, A.M. Brendzel, A. Blum, Chem. Phys. 57 (1981) 147–155.
[18] D.N. Nikogosyan, H. Görner, J. Photochem. Photobiol. B: Biol. 13 (1992) 219–234.
[19] F. Gai, R.L. Rich, J.W. Petrich, J. Am. Chem. Soc. 116 (1994) 735–746.
[20] F. Gai, R.L. Rich, J.W. Petrich, J. Am. Chem. Soc. 116 (1994) 8859.
[21] M. Shirom, G. Stein, J. Chem. Phys. 55 (1971) 3372–3378.
[22] E.J. Hart, M. Anbar, The Hydrated Electron. Wiley, New York, 1970.
[23] E.J. Hart, J.W. Boag, J. Am. Chem. Soc. 84 (1962) 4090–4095.
[24] L.I. Josimovic, I. Jankovic, S.V. Jovanovic, Radiat. Phys. Chem. 41 (1993) 835–841.
[25] D. Creed, Photochem. Photobiol 39 (1984) 537–562.
[26] R.V. Bensasson, E.J. Land, T.G. Truscott, Flash Photolysis and Pulse Radiolysis. Pergamon Press, Oxford, 1983.
[27] W.G. McGimpsey, H. Görner, Photochem. Photobiol. 64 (1996) 501–509.
[28] L. Stryer, Biochemistry, 4th Edition, W.H. Freeman, San Francisco, 1995.
[29] H.B. Steen, J. Chem. Phys. 61 (1974) 3997–4002.
[30] J. Zechner, G. Köhler, N. Getoff, I. Tatischeff, R. Klein, Photochem. Photobiol. 34 (1981) 163–168.
[31] J.K. Thomas, S. Gordon, E.J. Hart, J. Phys. Chem. 68 (1964) 1524–1527.
[32] J. Cygler, G.R. Freeman, Can. J. Chem. 62 (1984) 1265–1270.
[33] M. Faraggi, A. Bettelheim, Radiat. Res. 72 (1977) 81–88.
[34] R.C. Armstrong, A.J. Swallow, Radiat. Res. 40 (1969) 563–579.
[35] S. Gorden, E.J. Hart, M.S. Matheson, J. Rabani, J.K. Thomas, J. Am. Chem. Soc. 85 (1963) 1375–1377.
[36] K.J. Laidler, Chemical Kinetics, 2nd Edition, McGraw-Hill, New York, p. 10, 1965.
[37] J.Y. Lee, J.F. Baugher, L.I. Grossweiner, Photochem. Photobiol. 29 (1979) 867–874.